NaK-Nitrogen Liquid Metal MHD Converter Tests at 30 kw

D. J. CERINI*
Jet Propulsion Laboratory, Pasadena, Calif.

A NaK-nitrogen liquid metal MHD converter was operated over a range of nozzle inlet pressures of 100 to 165 N/cm², NaK flowrates of 46 to 72 kg/sec, and nitrogen flowrates of 2.4 to 3.8 kg/sec. The generator was operated as an eight-phase linear induction generator with two of the eight phases providing magnetic field compensation to minimize electrical end losses at the generator channel inlet and exit. Each of the eight phases was connected to a separately controlled capacitor bank for magnetization reactive power and a separately controlled load bank for dissipation of the output power. Generator operation was obtained with average winding currents and voltages up to 80 amp and 500 v, respectively, with estimated channel magnetic fields up to 0.4 T over the range of frequencies of 270–470 Hz. The output power of the converter was varied from −6 to 31 kw. At maximum output, the winding losses, fluid friction losses, and fluid ohmic losses were estimated to be 18, 21, and 49 kw, respectively, for a sum of 119 kw extracted from the fluid corresponding to net and gross efficiencies of 31/119 = 0.26 and (31 + 18)/119 = 0.41, respectively.

I. Introduction

THE purpose of the converter experiment was to demonstrate the feasibility of electrical power generation with an ambient temperature liquid metal magnetohydrodynamic (LM-MHD) separator cycle. The test unit contained all the principal components of what is called an MHD converter. There are four such components in the separator-type MHD converter in contrast to the other three converter types, which are the injector-condenser, emulsion, and slug-flow cycles.[1]

A high-temperature (LM-MHD) separator cycle operates at 1000°C by accelerating liquid lithium with cesium vapor through a linear induction generator to produce electric power.[2] Studies of space power applications have shown cycle efficiencies ranging from 5% up to 14%. Recent studies have also identified LM-MHD as a means of significantly improving the efficiency of land-based steam turbine power systems.[3]

The features of LM-MHD technology to be demonstrated in this first experimental system test were those of conversion of kinetic energy of a closed-loop liquid metal flow by means of a linear induction generator. Since these embody the hydraulic and electrical design features of an MHD space power plant, the demonstration could adequately and more easily be demonstrated in a test without the high temperature and material requirements associated with MHD converter tests with cesium and lithium; gaseous nitrogen and NaK (eutectic alloy of sodium and potassium) were thus chosen to simulate the closed-loop liquid metal flow of an MHD converter with power generation.

II. Converter Description

Figure 1 shows the final test configuration of the NaK-nitrogen converter. The four components are summarized below.

Nozzle

The nozzle assembly performs two primary functions: atomization and acceleration of the electrical working fluid (NaK). The atomization is achieved by the mutual impingement of the NaK and the gaseous nitrogen in the form of 1500 individual jets. Fine atomization of the liquid is a key parameter that determines the nozzle performance, the most important aspect of performance being the degree which the nozzle exit velocity can be made to approach the isentropic exit velocity. Reference 4 contains the analysis, design, and performance summary for the nozzle used in the NaK-nitrogen converter.

Separator

The separator is a 13.4-cm-high by 15.4-cm-wide by 60-cm-long flow duct placed between the nozzle exit and MHD generator inlet for the purpose of raising the stagnation pressure of the electrical working fluid as well as regaining the electrical conductivity lost in the acceleration of the NaK. This is achieved by coalescence of the liquid flow by impingement along the separator wall. Reference 5 summarizes the separator development program.

Generator

The generator components and diffuser inlet are shown in Fig. 2 prior to assembly. The upper stator is shown in position ready to be assembled with the lower stator. The stators are fabricated from 0.35-mm-thick, 2% silicon-iron laminations

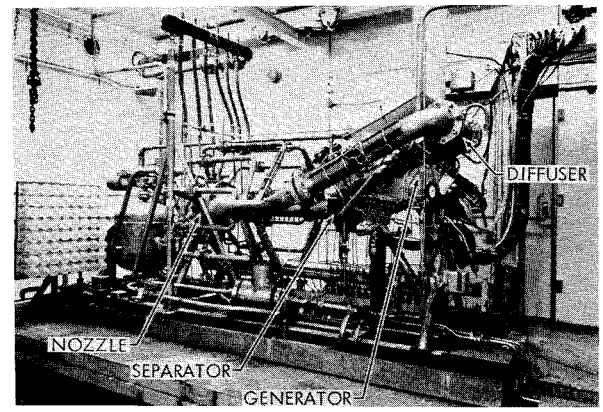

Fig. 1 NaK-nitrogen converter test installation.

Received March 26, 1973; revision received August 2, 1973. This work presents the results of one phase of research carried out in the Propulsion Research and Advanced Concepts Section of the Jet Propulsion Laboratory, California Institute of Technology, under Contract NAS7-100, sponsored by NASA.

Index categories: Multiphase Flows; Plasma Dynamics and MHD; Spacecraft Electric Power Systems.

* Member Technical Staff. Member AIAA.

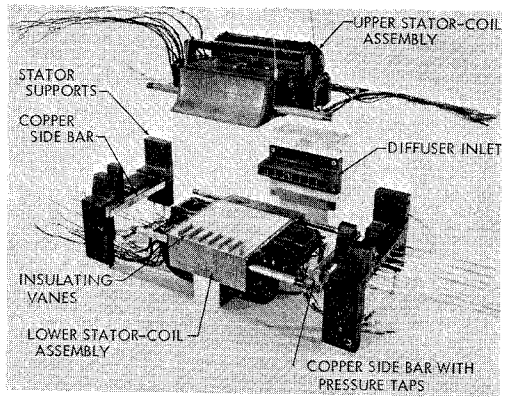

Fig. 2 NaK-nitrogen generator components.

bonded to form a 6.3-cm-high by 16.6-cm-wide by 20.5-cm-long block. The stator coil slots were machined after bonding. The copper sidebars are 10.9 cm long with a 1.28- by 1.3-cm cross section and are used to provide a low resistance path, parallel to the flow direction, for the electrical fluid currents. The sidebars extend into the gap between the two stators to form the sides of the flow channel. The inlet of the generator flow channel contains seven 0.10-cm-thick insulating vanes to reduce the ohmic losses in the compensating pole region. The diffuser inlet which is placed between the downstream compensating poles contains vanes for the same reason. The flow channel width is constant at 15.4 cm between the copper sidebars. The height of the flow channel varies over the length of the generator channel as shown in Fig. 3. The flow channel height and iron gap decrease from 1.25 cm to 1.03 cm over the 4.57-cm length of the upstream compensating pole. The iron gap in the power generating region is constant at 1.30 cm, whereas the flow channel height increases linearly from 1.03 to 1.3 cm over the 10.88-cm length of the power region. The iron gap increases from 2.5 cm to 3.0 cm over the length of the downstream compensating pole, whereas the flow channel walls diverge with a 3.75° half-angle from 1.30 cm to 5.22 cm to form the 29.67-cm-long diffuser channel. The diffuser inlet section contains the insulating vanes and is made of a nonmetal, fiberglass, to eliminate eddy current wall losses.

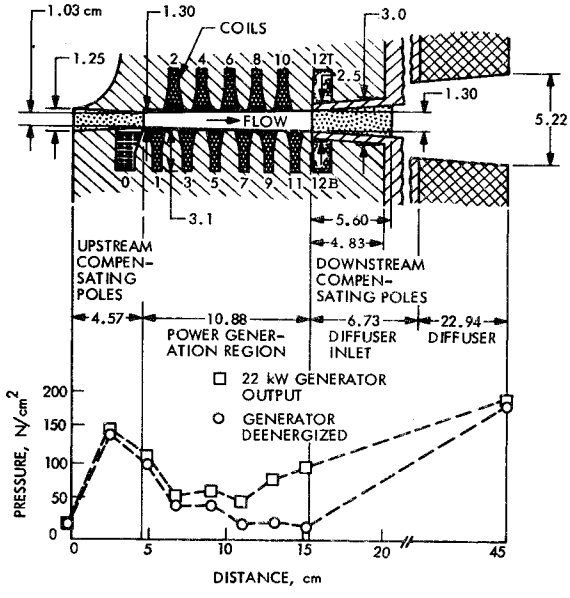

Fig. 3 Generator stator geometry with experimental channel pressure profile.

Table 1 MHD generator winding summary

Phase No.	Winding sequence slot number	Number of turns	Conductor diameter, mm	dc coil resistance, Ω	ac/dc resistance ratio at 350 Hz
1	1 to 7[a]	45	1.59	0.224	1.92
2	2 to 8	45	1.59	0.238	2.56
3	3 to 9	45	1.59	0.251	2.51
4	4 to 10	45	1.59	0.265	2.2
5	5 to 11	45	1.59	0.285	2.17
6	6	45	1.59	0.219	3.6
7	0	55	1.59 × 3.18 (rectangular)	0.091	4.1
8	12T, 12B	55	1.59	0.479	3.17
Average					2.78[b]

[a] Refer to Fig. 3 for slot number locations.
[b] An over-all value of 2.84 was measured in empty channel winding tests.

The MHD generator design uses an end-loss-compensated type single wavelength winding. See Ref. 6 for a discussion of MHD generator end loss compensation. The electrical power generation comes about by the conversion of flow kinetic energy directly to electrical power inductively transferred to the stator windings. The generator design is basically the same used in the intial tests of the converter.[7] The stator slots were changed by increasing the width and depth approximately 10% to allow for additional coil insulation. The flow channel was changed by eliminating the 0.14-cm outward step in the walls at the exit of the upstream compensating pole (Fig. 3 in Ref. 7). The generator windings were modified to increase reliability and decrease the ac winding losses over the coils used in initial tests. Magnet wire with a 0.04-mm film insulation was used to wind the nine coils required to form the eight phases as summarized in Table 1. Four individual coils were used in slots 0, 6, 12T, and 12B with end turns being completed around the back of the stator. To minimize end turn length, the other five coils were wound slot to slot. Increased dc coil resistances were accepted in this winding design to allow for additional insulation to overcome coil-to-ground and turn-to-turn insulation failures as a result of winding excitation with direct exposure to liquid metal. To meet this environmental operating requirement a minimum coil acceptance standard was adopted, that of 10-MΩ resistance to ground at 1000 v ac with the coil immersed in a 15 μΩ-cm electrolyte, followed by a power loss measurement at 80 amp in the test stator at temperatures up to 150°C. The coils were vacuum-impregnated with an epoxy insulating material after winding and again after installing all coils into the stator slots.

Each of the eight winding phases was connected to a variable capacitor bank to provide the reactive magnetization power. A rotating alternator was connected across phase 7 to provide power input required for startup and empty-channel tests. The other seven phases had load resistors for output power dissipation. The generator wiring schematic is the same as in the previous converter tests described in Fig. 6 of Ref. 7.

Diffuser

The diffuser assembly consists of the vaned diffuser inlet section described above plus the diffuser weldment shown in Fig. 1. This section accomplishes the final flow kinetic energy conversion to pressure before the flow leaves the diffuser through the two 12.5-cm-diam pipes at a velocity of approximately 5 m/sec and a pressure of 10 N/cm² above the mixer inlet pressure.

III. Empty-Channel Tests

The first part of the generator empty-channel test was conducted to measure the generator "impedance matrix." This matrix is an eight-by-eight array of complex coefficients which

when multiplied by a column matrix of the eight winding current vectors gives a column matrix of the eight winding voltage vectors as would be measured in an empty-channel test,

$$\begin{bmatrix} V_1 \\ V_2 \\ \vdots \\ V_8 \end{bmatrix} = \begin{bmatrix} Z_{11} & Z_{12} & \cdots & Z_{18} \\ Z_{21} & \cdots & \cdots & Z_{28} \\ \vdots & \vdots & & \vdots \\ Z_{81} & \cdots & \cdots & Z_{88} \end{bmatrix} \times \begin{bmatrix} I_1 \\ I_2 \\ \vdots \\ I_8 \end{bmatrix} \quad (1)$$

or

$$V = ZI \quad (2)$$

This relationship will then be used to calculate the fluid currents I_f in a power generation test where the vector currents in the matrix I above are the vector sum of the winding and fluid currents. Thus

$$I_f = Z^{-1} * V - I_w \quad (3)$$

The procedure for obtaining this impedance matrix is described in Ref. 7.

The second half of the empty-channel test was conducted to obtain winding loss as a function of winding current amplitude I_w and frequency f. The result was

$$P_w = \sum_{n=1}^{8} |I_w|^2 R_n(1+6.5f^{1.2}) \quad (4)$$

where R_n is the dc phase resistance in Table 1 and f is in kHz. This was obtained by measuring the total power input to the eight phases over a range of operating frequencies of 270 to 450 Hz, with each of the eight winding current vectors set to match the desired total current vectors in a fully compensated power test. Such a condition requires: 1) equal amplitude and 30° phase spacing between phase currents 1 to 6; 2) currents 7 and 8 phase angles of 122° lagging and 121° leading vector 6, respectively; and 3) currents 7 and 8 amplitude of 2.09 and 0.91 times the amplitude of current 1, respectively.

IV. Converter Experimental Program

The primary aspect of converter performance investigated was that of electrical power generation over a range of hydraulic operating conditions. This was performed in a series of 24 combined flow and power tests with the last three being run in a self-excited mode. The flow duration in each test was limited to approximately 5 min by the amount of nitrogen available for maintaining closed-loop NaK flow. The equipment and operations were the same used in the previous test series,[7] but the duration of the generator test was reduced to the minimum time required for data acquisition in order to minimize winding thermal stresses. A typical test consisted, first, of setting the capacitance and load values across each phase as calculated to be required for the particular flow conditions to be set. The flow was then started and the operating conditions of nozzle inlet pressure and nozzle liquid-to-gas mass flow ratio were set by adjusting the NaK inventory control regulator and the nitrogen flow regulator, respectively. The generator was then started by energizing the eight-phase winding to a particular current level as controlled by the phase 7 alternator excitation. The data was recorded and the generator stopped by disconnecting the alternator. During the 5-min flow duration a series of up to seven such generator tests were made over a range of frequencies and winding current levels. The first six runs of the test series were conducted at nozzle inlet pressures of 100 to 130 N/cm^2 and winding currents up to 50 amp to verify the ability to set balanced winding currents on the six power generating phases with approximately the predicted output power. The remaining runs were conducted at the design flow conditions of 158 N/cm^2 nozzle inlet pressure. The nitrogen flowrate was maintained in the 3.3 to 3.6 kg/sec flowrate range; outside this range large pressure increases occurred at the upstream or downstream ends of the generator channel.

Over the next 15 runs, capacitance, load, and winding current increases were made until operation was obtained at the design condition of 30-kw net output power and 80-amp average winding current. The final three runs were conducted to investigate the self-excitation capabilities of the generator.

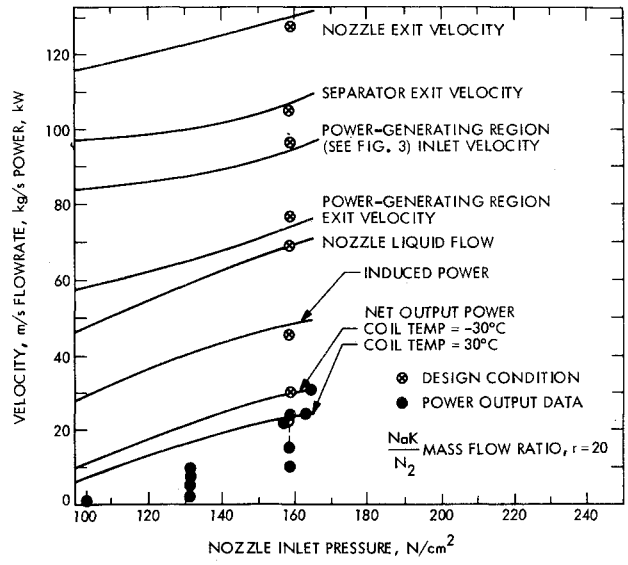

Fig. 4 Variation of converter velocity, flowrate, and power with nozzle inlet pressure.

V. Converter Performance

The test goal for the converter test was 30-kw output power at a frequency of 350 Hz and winding current of 70 amp. The flow conditions expected to be required were a nozzle inlet pressure of 158 N/cm^2, NaK flowrate of 69 kg/sec, and generator inlet and exit velocities of 96 and 76 m/sec, respectively.

Nozzle-Separator

Three of the primary performance parameters, nozzle and separator exit velocities, and liquid flowrate, could not be measured directly. However, from measurements of the nitrogen flowrate and nozzle inlet pressure, with the aid of open-loop calibration data, it was possible to calculate the nozzle exit velocity and liquid flowrate by means of the analysis of Ref. 5. The variation of calculated nozzle exit velocity and liquid flowrate with nozzle inlet pressure is shown in Fig. 4. The design-condition nozzle exit velocity is slightly below the calculated value for the tests because the measured nozzle exit pressure was 16 N/cm^2 instead of the 18 N/cm^2 assumed at the design condition.

The separator performance is summarized in Fig. 4 also. The separator exit velocity is calculated as described in Ref. 5. The liquid flow loss with the nitrogen exhaust flow is a directly measurable separator performance parameter. It ranges from 1.0% to 1.9% of the nozzle flow, which is within the goal of 2% while achieving a reduction in flow r_v (ratio of gas to liquid volume) from 21.4 at the nozzle exit to 1.4 at the separator exit. This represents a factor of 10 increase in electrical conductivity for the flow through the separator as calculated for the separator exit conditions from

$$\sigma/\sigma_L = (1+r_v)^{-n} \quad (5)$$

where σ/σ_L is the ratio of mixture to pure liquid conductivity as a function of volume ratio. The nozzle exit conductivity ratio is estimated to be 0.02 at an r_v of 21.4 (Fig. 3 of Ref. 8). For the separator exit conductivity calculation a value of $n = 2$ was used in Eq. (5), which lies between the value from the previous converter data[7] and the earlier correlation,[9] both of which are shown in Fig. 5. The conductivity increase through the separator is achieved at the expense of flow velocity. Figure 4 shows the velocity at the separator exit to range from 81% to 85% of the

Table 2 Electrical and flow conditions at maximum power

Flow Rates	
Nitrogen	3.6 kg/sec
NaK	70.5 kg/sec[a]
NaK entrained with nitrogen exhaust	1.3 kg/sec
Pressures	
Mixer inlet	174 N/cm^2
Nozzle inlet	164 N/cm^2
Nozzle exit	16 N/cm^2
Separator exit	20 N/cm^2
Upstream diffuser exit	74 N/cm^2
Generator channel average	70 N/cm^2
Downstream diffuser exit	190 N/cm^2
NaK Velocities	
Mixer inlet	5 m/sec[a]
Nozzle exit	132 m/sec[a]
Separator exit	109 m/sec[a]
Traveling wave inlet	96 m/sec[a]
Downstream diffuser inlet	76 m/sec[a]
Electrical Conditions	
Frequency, f	292 Hz
Average traveling wave field, B	0.404 T, rms[a]
Upstream compensating pole field, B_{C1}	0.160 T, rms[a]
Downstream compensating pole field, B_{C2}	0.032 T, rms[a]
Side plate voltage, V_{SP}	1.97 v, rms
Output power, P_e	31.2 kw
Winding power, P_w	17.2 kw[a]
Induced power, $P_i = P_e + P_w$	48.4 kw[a]

[a] Calculated values.

nozzle exit velocity. A factor of 4 increase in isentropic stagnation pressure was calculated for the flow through the separator.

Generator-Diffuser

Generator operation above the 10-kw net output power level was obtained for a total of 2.6 min, above the 20 kw level for 1.4 min, and above the 30-kw level in the one run summarized in Tables 2 and 3. This run was at a nozzle inlet pressure of 164 N/cm^2, slightly above the design pressure of 158 N/cm^2 as shown in Fig. 4, but the increase from the 24-kw output level obtained in several prior runs was due to reduced winding losses produced by pretest cooling of the generator to −30°C. The windings were precooled as an expedient to reduce the high dc winding losses in lieu of building low-loss coils that are relatively difficult and expensive to fabricate. The induced power (power output plus winding loss), calculated as in Ref. 7, was unchanged for the test with and without cooling.

Figure 3 shows the generator channel measured static pressure profile in a run at 23 kw. The pressure rise in the upstream compensating pole from 20 to 100 N/cm^2 without excitation and 20 N/cm^2 to 108 N/cm^2 with excitation is produced by the

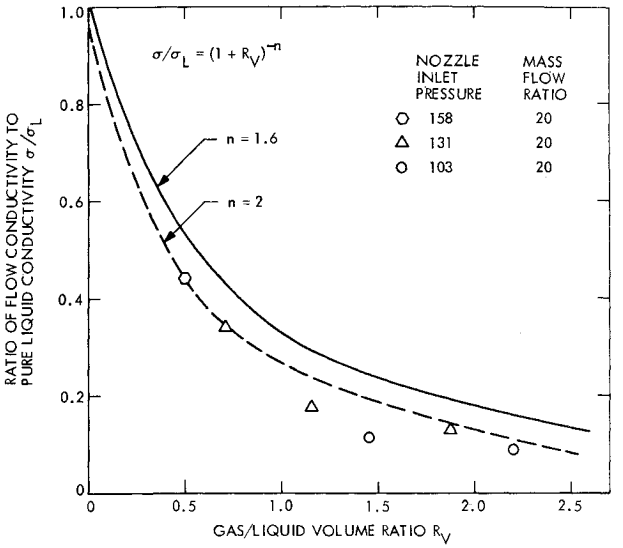

Fig. 5 Fluid conductivity as a function of generator gas/liquid volume ratio.

convergence of the stator surfaces in this region for the purpose of r_v decrease and thus conductivity increase. The pressure rise to 145 N/cm^2 at 3 cm may not be representative of the main-flow channel pressure at this location, since the particular pressure tap sees only the portion of the flow between the outermost insulating vane and the channel sidewall. With excitation, the average pressure in the power generating region is 70 N/cm^2, which is the value used in calculating the generator channel flow conditions.[5]

Net Power Output

The measured net power output is shown in Fig. 6 as a function of channel magnetic field. The field is calculated from the sum of winding and fluid currents, estimated by multiplying the measured phase vector voltage by the inverse of the impedance matrix [Eq. (3)]. At the lower nozzle inlet pressure of 130 N/cm^2, the output power varied with the square of the magnetic field up to a power output of 9.5 kw and field of 0.33 T. A further increase in winding current reduced the output power as a result of flow changes and increasing magnetic saturation. This same characteristic is seen at the 158-N/cm^2 nozzle inlet pressure and 350-Hz frequency. The variation of output power between the three groups of data at this flow condition is produced by generator load variations. At the field of 0.39 T the output was increased from 12.5 to 19.1 to 22.6 kw by increasing the average load conductance across phases 1 through 6 from 0.025 to 0.032 to 0.048 S†, respectively. With

Table 3 Generator phase conditions

	Phase							
Parameter	1	2	3	4	5	6	7	8
Winding current, amp, rms	87.5	65.4	74.6	85.9	99.1	54.9	96.2	57.8
Winding current angle, deg	25	64	92	115	158	180	−53	77
Total current, amp, rms[a]	52.0	43.4	51.0	67.4	73.9	41.0	87.8	39.1
Total current angle, deg	6	41	85	97	156	178	−56	67
Fluid current, amp, rms[a]	41.8	30.9	25	30.9	25.5	13.9	9.3	20.5
Fluid current angle, deg[a]	−131	−82	−72	−20	−15	6	149	−84
Terminal voltage, v, rms	358	346	352	407	413	331	242	278
Output power, kw	6.60	5.99	5.71	8.86	9.13	5.55	−13.70	3.07

[a] Calculated values.

† Siemens unit of conductance.

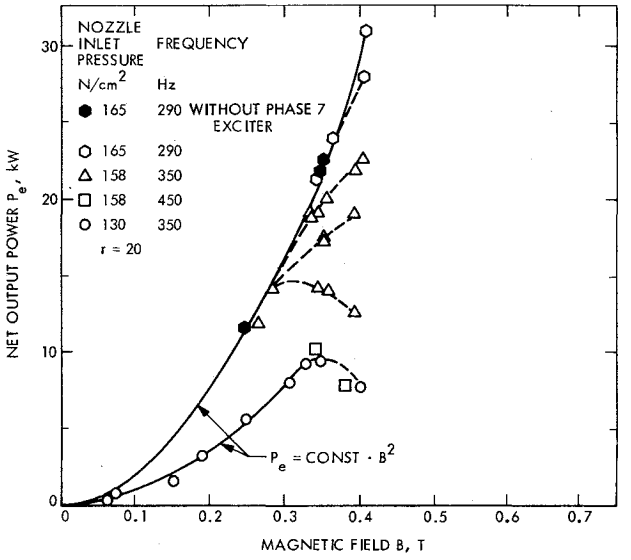

Fig. 6 Experimental net output power as a function of calculated rms magnetic field.

a change in operating frequency to 450 Hz with 0.016 S loading, the output power was reduced below 10 kw. At the highest nozzle inlet pressure and a generator load of 0.056 S, the peak output power of 31 kw was obtained with the generator precooled. At the end of this particular test, the heating of the coils had increased the average coil temperature from −30 to −11°C with a reduction in output power to 28 kw.

The calculated fluid input power available to the power generating region is $\dot{m}(V_1^2 - V_2^2)/2 = 119$ kw, where $\dot{m} = 69.2$ kg/sec is the mass flowrate in the generator channel, $V_1 = 96$ m/sec is the inlet velocity, and $V_2 = 76$ m/sec is the minimum velocity required for flow return through the diffuser to the nozzle. With 31-kw net output power, the over-all efficiency is $31/119 = 0.26$. Using the estimated winding losses of 18 kw gives a gross efficiency of $(31+18)/119 = 0.41$.

Fluid Conductivity

The electrical conductivity of the two-phase flow in the generator channel was calculated assuming the dependence of conductivity on liquid volume ratio given by Eq. (5). The values of conductivity were then used to calculate the theoretical output power at the nozzle inlet pressures of 130 and 158 N/cm². Good agreement was obtained between the calculated output power and the maximum measured output powers at these conditions where the generator channel volume ratio was estimated to be 0.7 and 0.5, respectively.

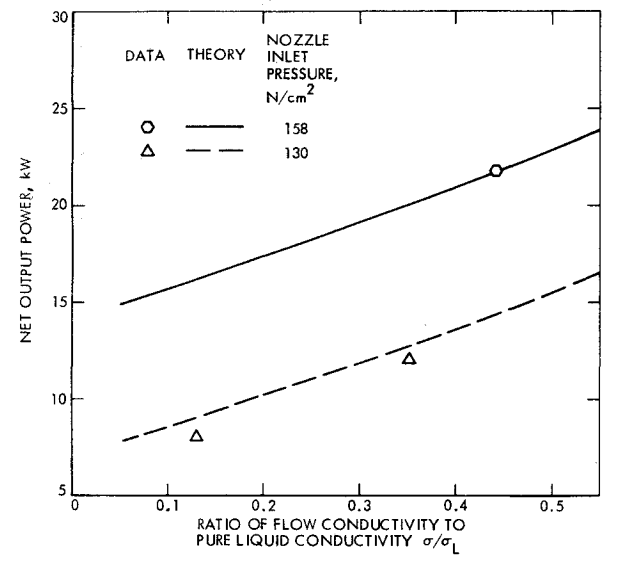

Fig. 7 Effect of channel flow conductivity on generator output power.

A value of $n = 2$ gives corresponding flow conductivity values of 0.35 and 0.44 times the pure liquid conductivity as shown in Fig. 5. This correlation is seen to agree with the previous NaK-nitrogen converter test data.[7] The earlier correlation[9] with an exponent value of $n = 1.6$ predicts conductivities 20% higher at a volume ratio of 0.5. The lower conductivity values in the NaK-nitrogen converter tests are considered to be produced by the wakes behind the vanes.

For a particular run at 158 N/cm² nozzle inlet pressure and frequency of 350 Hz, the output power was 22 kw at a conductivity ratio of 0.44 as shown in Fig. 7. The solid line through this data point shows the variation of calculated output power with both input power and volume ratio held constant. A conductivity increase from 0.44 to 0.53 corresponding to an exponent n decrease from 2 to 1.6 shows a 9% power increase from 22 to 24 kw. At the condition of maximum output power this power increase comes about because of reduced winding losses. The dashed curve in Fig. 7 shows the results for a similar calculation of output power at a nozzle inlet pressure of 130 N/cm². The data point at 12 kw and 0.35 conductivity ratio represents the maximum power condition at 130 N/cm.[2] The power data is normalized to a field of 0.39 T in order to show the previous power data[7] of 8 kw at a conductivity ratio of 0.13. Although both tests were at the same nozzle flow conditions, the slightly larger flow channel and higher flow velocities (due to low power level) of the earlier test account for the significantly lower flow conductivity.

Self-Excitation Generator Tests

The final three converter tests were conducted with phases 4 and 5 providing the power input to phase 7. This was accomplished by transformer addition of phases 4 and 5 winding currents. The resultant current vector was adjusted in phase angle and amplitude by means of a multitap dual primary transformer, such that it provided the desired input to phase 7. In the first test it was found that all the winding currents rose to an average of 65 A in a fraction of a second upon raising the nozzle inlet pressure above the 135 N/cm² level. Subsequent tests were conducted with the phase 7 capacitor bank short-circuited until the desired flow conditions were set, and then generator operation was obtained by removal of the capacitor-bank short circuit. The generator was operated above the 20-kw output power level for demonstration purposes with the load resistors on four of the phases replaced by the light-bulb bank shown in Fig. 1. The over-all performance of the converter can be summarized as excellent in that the over-all test goal was met indicating that the individual component performances were also at their design level.

VI. Conclusions

The most significant aspects of the NaK-nitrogen converter tests were: 1) smooth and stable operation of the combined hydraulic and linear induction MHD generator systems; 2) absence of unexpected electrical or flow losses; 3) operation of the converter at the design conditions of liquid metal and nitrogen flow with the full output power of 30 kw expected for those conditions.

References

[1] Morse, F. H., "Survey of Liquid Metal Magnetohydrodynamic Energy Conversion Cycles," *Energy Conversion*, Vol. 10, Pergamon Press, New York, 1970, pp. 155–176.

[2] Elliott, D. G., "MHD Power Systems," *Journal of Spacecraft and Rockets*, Vol. 4, No. 7, July 1967, pp. 842–846.

[3] Phen, R. L. and Hays, L. G., *Liquid Metal MHD Technology*

Transfer Feasibility Study, Document 1200-59, May 18, 1973, Jet Propulsion Lab., Pasadena, Calif.

[4] Elliott, D. G. and Weinberg, E., *Acceleration of Liquids in Two-Phase Nozzles,* TR 32-987, July 1968, Jet Propulsion Lab., Pasadena, Calif.

[5] Cerini, D. J., "Circulation of Liquids for MHD Power Generation," *Electricity from MHD,* 1968, International Atomic Energy Agency, Vienna, 1968, pp. 2019–2033.

[6] Cerini, D. J. and Elliott, D. G., "Performance Characteristics of a Single Wavelength Liquid Metal MHD Induction Generator with End Loss Compensation," *AIAA Journal,* Vol. 6, No. 3, March 1968, pp. 503–510.

[7] Cerini, D. J. and Elliott, D. G., "Test Results of a NaK-Nitrogen Liquid Metal MHD Converter," *Fifth International Conference on MHD Electrical Power Generation,* Vol. III, International Atomic Energy Agency, Vienna, 1971, pp. 177–192.

[8] Elliott, D. G., Cerini, D. J., Hays, L. G., and Weinberg, E., "Liquid Metal MHD Power Conversion," *Supporting Research and Advanced Development,* Space Programs Summary 37-30, Vol. IV, Jet Propulsion Lab., Pasadena, Calif., Dec. 31, 1964, pp. 116–119.

[9] Elliott, D. G., Hays, L. G., Cerini, D. J., and Bogdanoff, D. W., "Investigation of a Liquid-Metal Magnetohydrodynamic Power System," Fifth Intersociety Energy Conversion Engineering Conference, Sept. 1970, AIAA, New York.

JANUARY 1974 AIAA JOURNAL VOL. 12, NO. 1

Effective Electrical Conductivity and Related Properties of a Nonequilibrium High Pressure MHD Plasma

G. BREDERLOW* AND K. J. WITTE*
Max-Planck-Institut für Plasmaphysik, Garching, Germany

This paper describes measurements of the effective electrical conductivity, the effective Hall parameter, the electron temperature and the electron number density made in an argon-potassium plasma over a wide range of current densities from 1 to 12 amp/cm^2, pressures from 2.1 to 8.2 bar and magnetic inductions from 1.1 to 3.6 Tesla at a gas temperature of 1800 °K and a seed fraction of 0.05%. The aim of these investigations is to find out how well the available theories describing the influence of the magnetic field on the plasma properties mentioned can reproduce the experimental data. The measurements showed that in the entire parameter range investigated the theory based on a quasilinear analysis of plane ionization waves and also a semiempirical model agree with the experiment within the measuring accuracy as far as the effective electrical conductivity, the electron temperature and electron number density are concerned.

I. Introduction

THE coupling between the current density and the electron density in a rare-gas-alkali plasma is the reason why it is not possible under MHD generator conditions (crossed electric and magnetic fields) to obtain a stable plasma configuration above a certain critical Hall parameter. Such a plasma is then subject to the discharge structures known as streamers, within which ionization instabilities develop. As outlined in more detail in Ref. 1 the streamers can be considered as zones of elevated current density compared with the corresponding uniform plasma, which are oriented parallel to the mean current direction and are caused by inhomogeneous boundary conditions (segmented electrodes). They are therefore a phenomenon different from the ionization instabilities which are a pure volume effect. Whereas the ionization instabilities reduce the effective electrical conductivity and lead to saturation of the Hall parameter, the streamers do not impair the plasma properties at least in the pressure range of $p \simeq 1$ bar investigated so far.[2] To ensure sufficient accuracy in calculating the performance of a generator in those parameter ranges in which it will have to be operated later in nuclear power stations, an essential requirement is to know the scaling laws for the effective electrical conductivity. For this reason the effective electrical conductivity was experimentally determined for various gas pressures, current densities and magnetic inductions. These results were compared with theoretical values to check which of the various theories describing the influence of ionization instabilities on σ_{eff} best approximates actual conditions. This comparison was taken further by making, at a constant gas pressure, spectroscopic measurements of the electron temperature and electron density as functions of the current density at various magnetic inductions.

Another question of interest here was whether the influence exerted by ionization instabilities on the effective electrical conductivity can be reduced by the streamers when the gas pressure is increased. This is because the extent of the streamers could be decreased on elevation of the pressure since the characteristic length describing the smallest region in which sharp gradients in the plasma properties can form decreases with rising pressure. In the streamers the current density and hence the degree of ionization as well could then increase. If the latter reaches the region of full ionization, it is to be expected that the influence of the ionization instabilities on the effective electrical conductivity will be reduced.

Received May 30, 1973; revision received August 10, 1973. The authors wish to express their gratitude to R. Borde, C. Geisreiter and J. Hartmann for construction of the apparatus and assistance in conducting the experiments. This work was performed under the terms of the agreement on association between Max-Planck-Institut für Plasmaphysik and Euratom.

Index categories: Atomic, Molecular and Plasma Properties; Plasma Dynamics and MHD; Electric Power Generation Research.

* Research Scientist.